Bound electron contribution to soft x-ray laser interferograms of dense plasmas

J. Filevich, J.J. Rocca, and M.C. Marconi*

NSF ERC for Extreme Ultraviolet Science and Technology

and Department of Electrical and Computer Engineering,

Colorado State University, Fort Collins, Colorado 80523

Livermore Authors

Lawrence Livermore National Laboratory, Livermore, California 94550

(Dated: April 15, 2004)

Abstract

We present experimental evidence showing that the contribution of bound electrons to the index of refraction can significantly affect soft x-ray laser interferograms of laser-created plasmas. We report picosecond resolution soft x-ray laser interferograms of Al laser-created plasmas that late in their evolution display negative fringe shifts in the plasma periphery. Simulated density maps show that this results from the dominant contribution of low charge ions to the index of refraction. If neglected, the presence of significant densities of low charge ions in laser-created plasmas may result in the overestimation of the measured electron density for most materials.

PACS numbers: 07.60.La (Interferometers), 42.87.Bg (Phase shifting Interferometers), 52.50.Jm (Plasma Heating by Laser beams)

Keywords:

*Permanent Address: Department of Physics, University of Buenos Aires, Buenos Aires, Argentina.

I. INTRODUCTION

Soft x-ray laser interferometry is a powerful new plasma diagnostics tool that is rapidly maturing. Several groups have produced results in recent years, using different interferometer schemes [1–4]. The advantages of using soft x-ray lasers for measuring electron densities in high density plasmas have been discussed in the literature [1]. They consist of significantly reduced refraction and free-free absorption that allow the measurement of larger and denser plasmas. Following the demonstrations of soft x-ray laser interferometry with laboratory size soft x-ray lasers, the development of compact discharge-pumped soft x-ray lasers has allowed the implementation of soft x-ray plasma interferometry in a table-top set up [2, 4, 5]. The recent demonstration of picosecond soft x-ray laser interferometry techniques [6, 7], with which plasma motion blurring can be reduced, allows the diagnostics of large scale laser-created plasmas at very small distances from the target surface.

The correct interpretation of the interferograms is key to obtaining an accurate representation of the electron density distribution. Since high density plasmas generated by intense laser beams tend to be highly ionized, the spatial distribution of the free electrons is usually obtained assuming that their contribution to the fringe shift is much larger than that of the bound electrons. This assumption, which has been utilized to analyze all soft x-ray laser interferometry studies of laser-created plasmas realized to date, is valid for hot plasmas but can fail as the plasma cools down and the mean degree of ionization of the plasma decreases.

In this paper we present interferometry data obtained with a picosecond 14.7 nm (84.4 eV) laser probe that shows clear evidence of the dominant contribution of bound electron s to the index of refraction in the late stages of the evolution of an Al plasma created by a high power laser. The interferograms show that at late times in the plasma evolution the fringes in the periphery of the plasma region irradiated by the heating laser bend toward the target (negative fringe shifts), as opposed to away from the target, as occurs at earlier times. Similar negative fringe shifts were also recently observed in an independently realized Al laser-created plasma soft x-ray laser interferometry experiment at 13.9 nm, but the results were not analyzed in detail[8]. Analysis of our data done with the assistance of hydrodynamic model simulations indicates that late in the plasma evolution the contribution of bound electrons dominates the index of refraction, causing the observed negative fringe shifts in the periphery regions of the plasma.

In phase shift interferometry the number of fringe shifts, given by $N_f = \frac{1}{\lambda}\int_0^L (1-\eta)dl$, is negative when the index of refraction (η) of the plasma is greater than 1. The contribution of the free electrons to the plasma index of refraction is always less than 1, as determined by $\eta = (1 - n_e/n_{crit})^{\frac{1}{2}}$ where $n_{crit} = 5 \times 10^{24} cm^{-3}$ is the critical density for $\lambda = 14.7$ nm. This suggests that the contribution from bound electrons to the index of refraction, in the region where negative fringe shifts are obseved, is dominant and to be greater than one. Of all the elements with atomic number less than 55, Al is the only one that has a negative f_1^0 real scattering factor at λ=14.7 nm, due to the close proximity of the L shell resonances to the 84.4 eV photon energy. This negative scattering factor that translates into a contribution to the index of refraction greater than one ($\eta = 1 - \frac{n_a r_e \lambda^2}{2\pi} f_1^0$ where n_a is the atom density and r_e is the classical electron radius) suggests that when the density of neutral and low charged Al atoms is sufficiently high the fringes will shift toward the target. It is expected that at this wavelength, this effect will only be present in Al plasmas. In fact, the effect was not observed in interferograms of plasmas we generated with very similar laser heating conditions using several other target materials (Ti, Cr, Pd, Mo, Au). Figure 1 shows a comparison of Interferograms for Al, Ti and Pd, all obtained at approximately the same time in the plasma evolution, $\approx$ 3 ns after the peak of the heating laser pulse. The Al interferogram shows negative fringe shifts on the periphery of the plasma while the interferograms corresponding to Ti and Pd show only positive fringe shifts.

In such cases in which the bound electrons make a significant contribution to the index of refraction, the electron density cannot be obtained directly from the interferometry data of a single interferogram, and more sophisticated techniques have to be used to deconvolve the contributions of free and bound electrons. In the probing of low electron density plasmas with optical lasers, two-color interferometry has been widely used to separate the contribution of free and bound electrons [**?**]. However, this technique has not yet been used at soft x-ray laser wavelengths where its implementation is difficult. Instead we analyze the contribution of bound and free electrons by making use of hydrodynamic simulations.

II. EXPERIMENT RESULTS AND ANALYSIS

The experiment was performed using a transient 14.7 nm Ni-like Pd soft x-ray laser [9] combined with an amplitude division diffraction grating interferometer (DGI)[2]. The inter-

ferometer is set in a skewed Mach-Zehnder configuration, with the principal distinguishing characteristic being the use of diffraction gratings as beam splitters. This results in a very robust scheme that can be adapted to operate at different soft x-ray wavelengths by choosing the proper grating's parameters. The DGI design produces interferograms with very good visibility over a large field of view, as first demonstrated with a 46.9 nm capillary discharge soft x-ray laser [2]. The Ni-like Pd soft x-ray laser used in this experiment produced laser pulses of few 10's of μJ with a typical duration in the range of 4.5 - 5.2 ps [10]. It was pumped by a sequence of a 600 ps FWHM, 2 J long pulse and a 13 ps FWHM **(please confirm)**, 5 J short pulse generated by the COMET chirped pulse amplification laser [9]. The short pulse was delivered onto the target using a traveling wave line focus configuration. The resulting short duration of the soft x-ray laser pulse permits the acquisition of "snap-shots" of rapidly evolving plasmas, overcoming the blurring of interference fringes that occurs when the electron density profile changes significantly during the duration of the probe pulse. The picosecond soft x-ray laser interferometry set up is described in more detail in a recent paper [7].

Figure 2 shows a series of interferograms of an expanding Al plasma. The plasma was created by focusing a 600 ps, 3 J, 1054 nm laser into a 3.1 mm long $\times$ 12 μm wide line focus on a 1 mm long flat Al target. The target was positioned for the plasma to intercept one of the arms of the interferometer, and the timing between the heating and probe beams was measured using a fast photodiode. The two frames corresponding to the earlier time of the plasma evolution (0 and 0.8 ns) show a rapid lateral expansion of the plasma together with the formation of an on-axis density depression. At these times the fringes shift away from the target, even in the central region of the plasma where the on-axis depression is observed. This two-dimensional feature was first observed in soft x-ray laser interferograms of laser-created Cu plasmas obtained with a 46.9 nm capillary discharge soft x-ray laser [11, 12]. Hydrodynamic simulations of those experiments with the code LASNEX [13] showed that the electron density minimum in the central region of the plasma is the result of pressure equilibrium between the irradiated plasma region and the low temperature side-lobes, created by plasma-radiation induced ablation of the surrounding target region. A detailed discussion on the processes responsible for the formation of the side-lobes and the central density depression are discussed in recent works [11, 12].

The last two frames in Fig. 2 show a plasma in which the region close to the target

presents increased absorption, an indication of a colder plasma. Also the fringes at the periphery of the plasma shift toward the target, something that requires a total index of refraction greater than 1. We computed the real component of the index of refraction for the different ions that might be present in the plasma ***(Add the scattering factor calculation paragraph)***. Table 1. lists the computed "effective" f_1 ***(Is there a better name for this?)*** values for AlI - AlXIV, that include the contribution of ions and free electrons, can be used to calculate the total plasma index of refraction $\eta = (1 - \frac{n_Z f_1}{n_{crit}})^{\frac{1}{2}}$, where n_Z is the density of ions with charge Z. All ions with charge up to Z=5 are computed to make a significant negative contribution to the index of refraction which corresponds to "effective" f_1 factors that differ from the number of free electrons corresponding to the ion. The negative values of f_1 for AlI-AlIV in Table 1 suggest that the negative fringe shifts observed at the late times are due to the presence of a relatively high densities of these low charge atoms. To confirm this interpretation, the LASNEX hydrocode was used to compute the ion density and electron density distributions. The simulations were conducted using the measured temporal and spatial profiles of the plasma heating beam, and the results were used in combination with the f_1 factors of table 1 to synthesize interferograms that could be compared to those in Fig. 2. Figures 3 and 4 show the LASNEX computed electron density (lineouts), the corresponding electron temperature maps (Fig. 3), and the average ion charge distributions (Fig. 4). The electron density distributions measured during the early expansion 0 ns and 0.8 ns delay in Fig 2, including the lateral expansion and on-axis depression, are well reproduced by the code. This indicates that the assumption that the free electrons dominate the contribution to the index of refraction is valid at the early times, as is expected from the fact that at those times the plasma is hot and only highly ionized species are present.

At later times, corresponding to the last two frames of Fig. 2, the simulations show that the degree of ionization in the plasma periphery decreases as the plasma cools, resulting in significant concentrations of AlII-AlIV ions present. In this case the LASNEX simulation results were used to synthesize the interferograms that are shown in Fig 5. These synthetic interferograms were calculated taking into account the contributions to the index of refraction from free electrons and Al ions using the "effective" f_1 factors of Table 1. and the electron density and ion density distributions computed with LASNEX. The calculated interferogram corresponding to 0.8 ns delay shows the central density depression and the

lateral expansion observed in the measurements, and the late interferograms (1.7 and 3.2 ns) show the observed negative fringe shifts in the periphery of the plasma, in good agreement with the experiment. The onset of the negative fringe shifts occurs earlier in the computed interferograms (0.5 ns after the peak of the laser pulse) than in the experiments (1.2 ns), which might be indicative of a discrepancy in the recombination rate. The results illustrate that the combination of soft x-ray laser interferometry measurements can provide very valuable information to validate plasma simulation codes.

It can be expected that interferograms of the late stages of the evolution of many other laser-created plasmas involving the use of other materials will also be significantly affected by the contribution of bound electrons. However, the relative contribution of bound electron scattering is not always clearly evident in soft x-ray interferograms because at these wavelengths the free and bound electrons often contribute with the same sign to the phase delay, resulting in an apparently denser plasma. The results presented herein highlight the importance of taking into account the contribution of bound electrons to the index of refraction in the interpretation of soft x-ray laser interferograms.

III. CONCLUSIONS

We have probed Al laser-crated plasmas with 14.7 nm soft x-ray laser interferometry, and observed negative fringe shifts in the periphery of the plasma at late times in the plasma evolution. The phenomenon, that was observed to occur only in Al plasmas, is attributed to the dominant contribution of bound electrons to the index of refraction. This interpretation is supported by the results of hydrodynamic simulations that predict the existence of large concentrations of low charged ions at the time and location of the negative fringe shifts. Synthesized interferograms calculated based on the computed electron and ion distributions are in good agreement with the experiment. The contribution of the low charge ions to the plasma's index of refraction is particularly evident in the Al plasmas because of the fact that at this wavelength (14.7 nm) the contribution of free and bound electrons to the fringe shifts have opposite signs. This is in contrast with most other elements, for which the contribution of bound electrons to the fringe shift is in the same direction to that of free electrons, and if neglected can result in an undetectable overestimation of the electron density when the degree of ionization of the plasma is low. The results show that soft x-ray

plasma interferometry constitutes a powerful tool for the study of dense plasmas and the validation of plasma simulation codes.

Acknowledgments

The authors would like to thank Albert Osterheld of LLNL for continued support of this work. This research was sponsored by the National Nuclear Security Administration under the Stewardship Science Academic Alliances program through DOE Research Grant # DE-FG03-02NA00062. Part of this work was performed under the auspices of the U.S. Dept. of Energy by the University of California, Lawrence Livermore National Laboratory through the Institute of Laser Science and Application, under contract No. W-7405-Eng-48. The CSU researchers also gratefully acknowledge the partial support of the NSF ERC Center for Extreme Ultraviolet Science and Technology, award number EEC-0310717.

---

[1] L. B. Da Silva, T. W. Barbee Jr., R. Cauble, P. Celliers, D. Ciarlo, S. Libby, R. A. London, D. Matthews, S. Mrowka, J. C. Moreno, et al., Physical Review Letters **74**, 3991 (1995).

[2] J. Filevich, K. Kanizay, M. C. Marconi, J. L. A. Chilla, and J. J. Rocca, Optics Letters **25**, 356 (2000).

[3] B. Rus, T. Mocek, A. Präg, M. Kozlovà, M. Hudeček, G. Jamelot, J.-C. Lagron, A. Carillon, D. Ros, D. Joyeux, et al., in 8^{th} *International Conference on X-Ray Lasers*, edited by J. Rocca (2002), vol. Lloyd's plasma interferometry, pp. 182–189.

[4] J. J. Rocca, C. H. Moreno, M. C. Marconi, and K. Kanizay, Optics Letters **24**, 420 (1999).

[5] C. H. Moreno, M. C. Marconi, K. Kanizay, J. J. Rocca, Y. A. Uspenskii, A. V. Vinogradov, and Y. A. Pershin, Physical Review E **60**, 911 (1999).

[6] R. F. Smith, J. Dunn, J. Nilsen, V. N. Shlyaptsev, S. Moon, J. Filevich, J. J. Rocca, M. C. Marconi, J. R. Hunter, and T. W. Barbee, Physical Review Letters **89**, 065004 (2002).

[7] J. Filevich, J. J. Rocca, M. C. Marconi, R. F. Smith, J. Dunn, R. Keenan, J. Hunter, S. Moon, J. Nilsen, A. Ng, et al., In Press, Applied Optics (2004).

[8] H. Tang, O. Guilbaud, G. Jamelot, D. Ros, A. Klisnick, D. Joyeux, D. Phalippou, M. Kado, M. Nishikino, M. Kishimoto, et al., Applied Physics B **In Press** (2004).

[9] J. Dunn, Y. Li, A. L. Osterheld, J. Nilsen, J. R. Hunter, and V. N. Shlyaptsev, Physical Review Letters **84**, 4834 (2000).

[10] J. Dunn, R. Smith, R. Shepherd, R. Booth, J. Nilsen, J. Hunter, and V. Shlyaptsev, in *SPIE Int. Soc. Opt. Eng. Proc*, edited by E. Fill (2003), vol. 5197, (in Press).

[11] J. Filevich, J. J. Rocca, E. Jankowska, E. C. Hammarsten, K. Kanizay, M. C. Marconi, S. J. Moon, and V. N. Shlyaptsev, Physical Review E **67**, 056409 (2003).

[12] J. J. Rocca, E. C. Hammarsten, E. Jankowska, J. Filevich, M. C. Marconi, S. Moon, and V. N. Shlyaptsev, Physics of Plasmas **10**, 2031 (2003).

[13] G. Zimmerman and W. Kruer, Comments Plasma Phys. Controlled Fusion **2**, 51 (1975).

Figure captions

1. Comparison of interferograms obtained 3 - 3.2 ns after the peak of the heating laser pulse for three different materials, at similar heating conditions (3 J lasing). Negative fringe shifts are only present in the Al plasmas.

2. Sequence of soft x-ray laser ($\lambda = 14.7$ nm) interferograms of Al line focus plasmas. The plasmas were generated by a 3 J heating beam focused to a 12 $\mu m \times 1$ mm line focus. The times are measured respect to the peak of the 600 ps heating pulse. Negative fringe shifts in the periphery of the plasma and close to the target are observed for the last two frames.

3. Sequence of simulated electron density and electron temperature maps computed using the LASNEX code for the irradiation conditions used to obtain the interferograms of Fig. 2.

4. Sequence of simulated electron density and mean ionization distribution maps computed using the LASNEX code for the irradiation conditions used to obtain the interferograms of Fig. 1.

5. Synthesized interferograms computed using the calculated electron and ion densities from Fig 3.

Aluminum fringe reversal/Tex-version/Figure 1.jpg

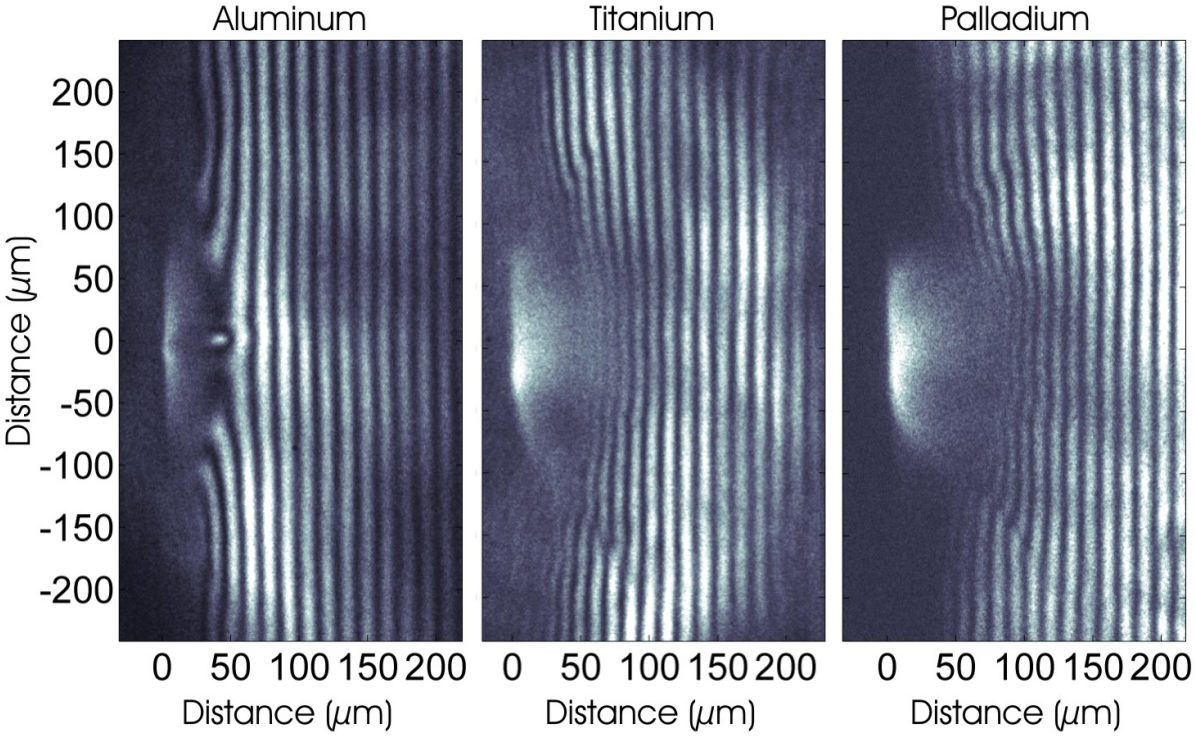

FIG. 1: Comparison of interferograms obtained 3 - 3.2 ns after the peak of the heating laser pulse for three different materials, at similar heating conditions (3 J lasing). Negative fringe shifts are only present in the Al plasmas.

Aluminum fringe reversal/Tex-version/Figure 2.jpg

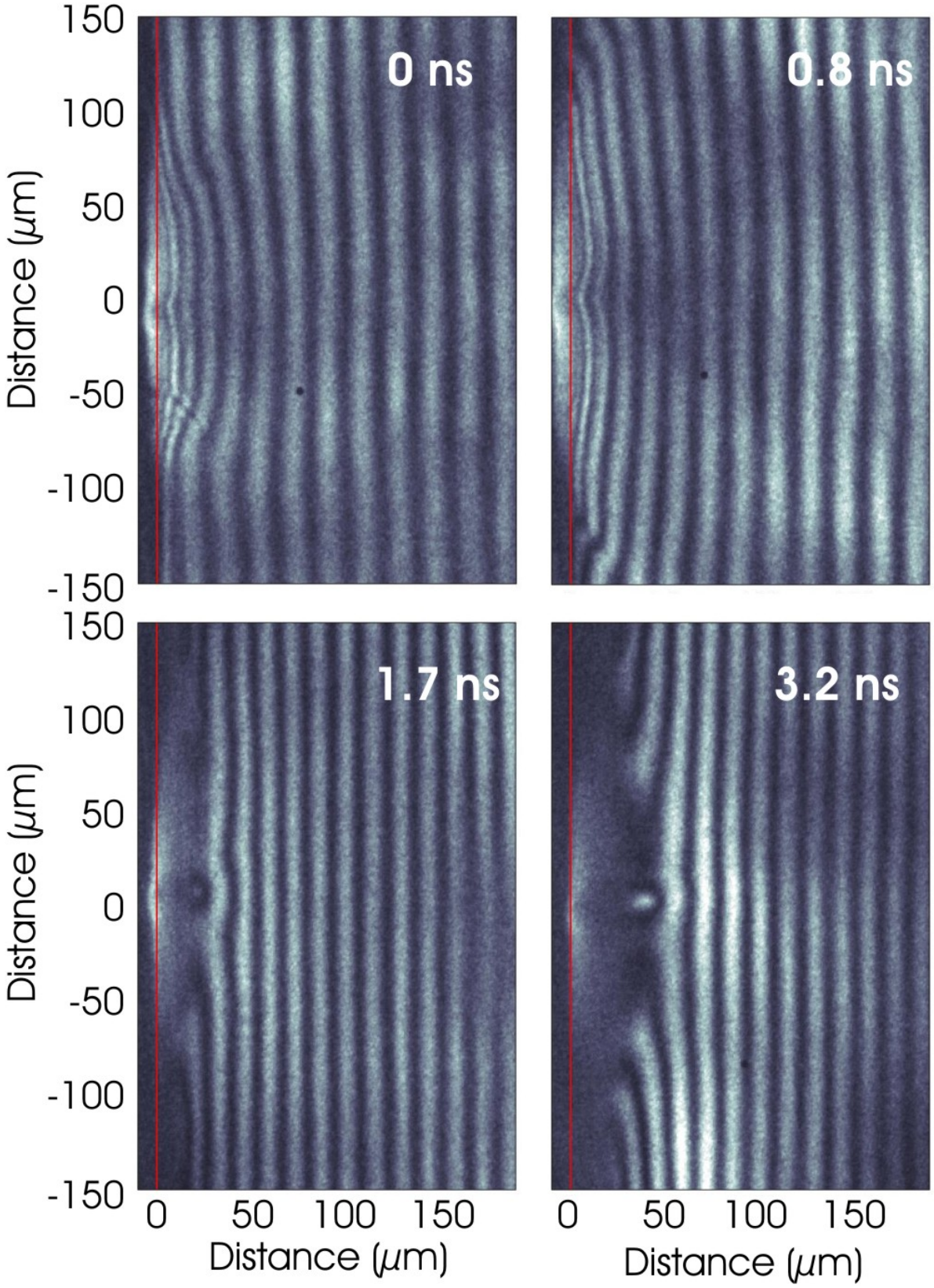

FIG. 2: Sequence of soft x-ray laser (λ = 14.7 nm) interferograms of Al line focus plasmas. The plasmas were generated by a 3 J heating beam focused to a 12 μm × 1 mm line focus. The times are measured respect to the peak of the 600 ps heating pulse. Negative fringe shifts in the periphery of the plasma and close to the target are observed for the last two frames.

Aluminum fringe reversal/Tex-version/Figure 3.jpg

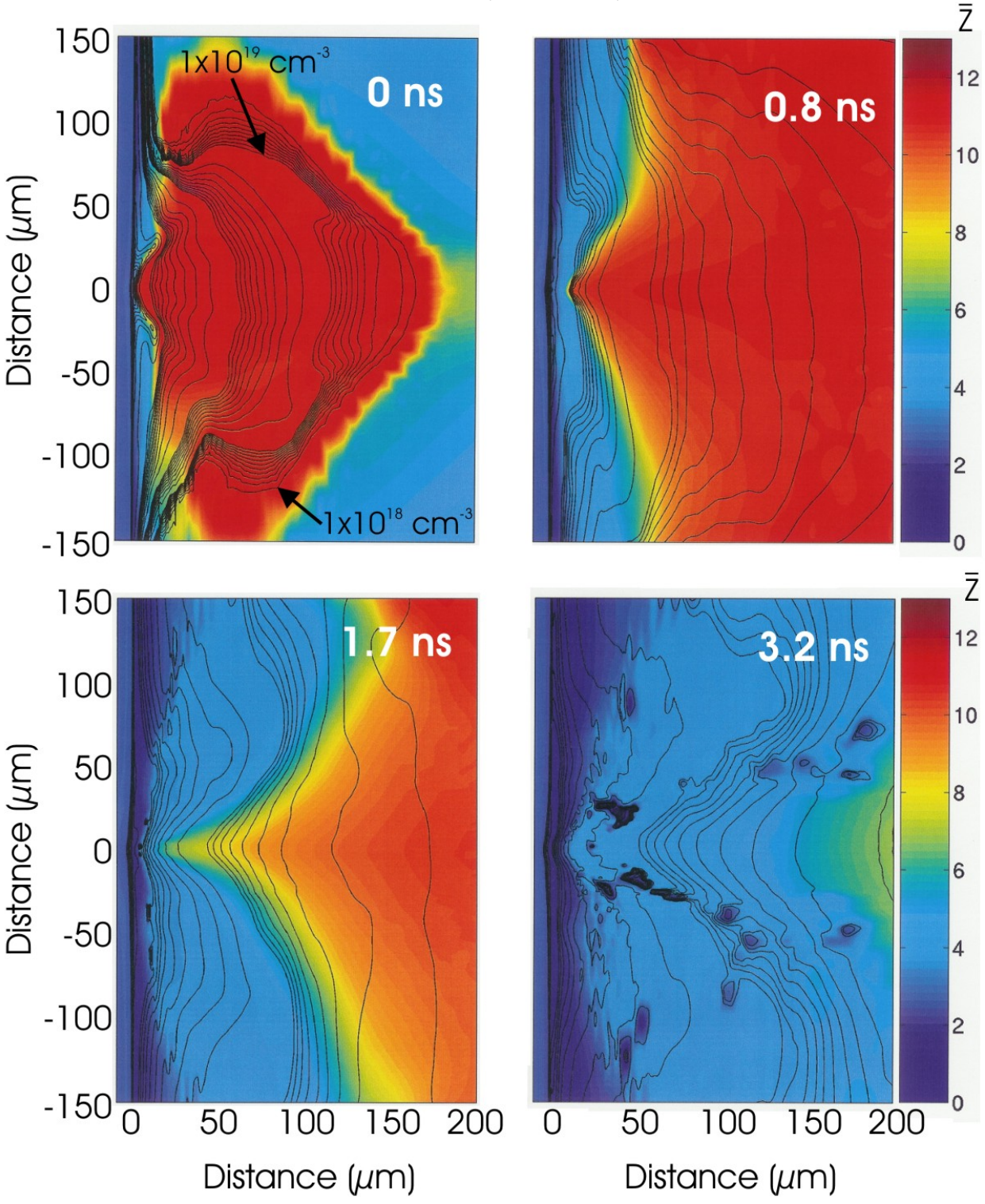

FIG. 3: Sequence of simulated electron density and electron temperature maps computed using the LASNEX code for the irradiation conditions used to obtain the interferograms of Fig. 2.

Aluminum fringe reversal/Tex-version/Figure 4.jpg

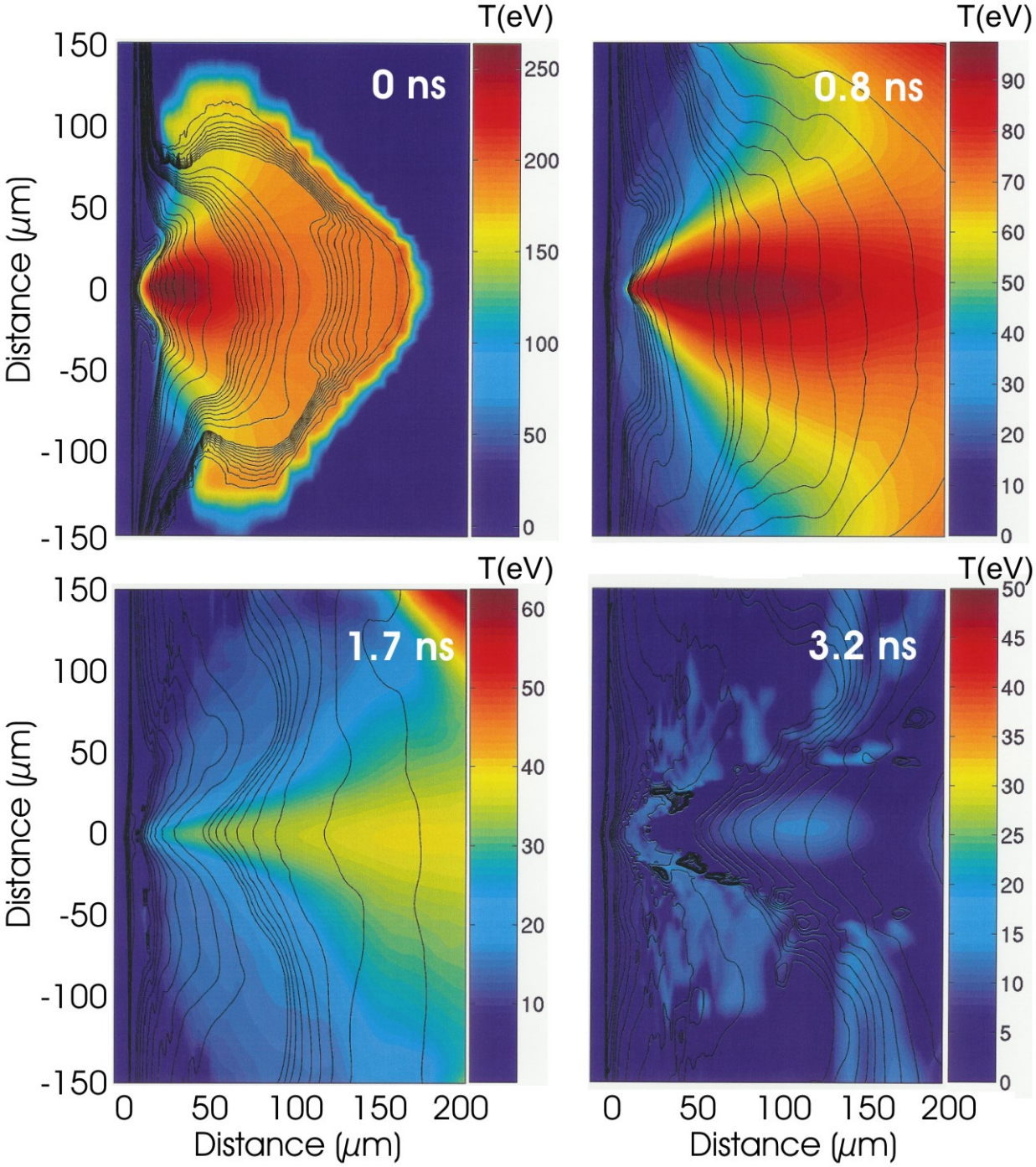

FIG. 4: Sequence of simulated electron density and mean ionization distribution maps computed using the LASNEX code for the irradiation conditions used to obtain the interferograms of Fig. 1.

Aluminum fringe reversal/Tex-version/Figure 5.jpg

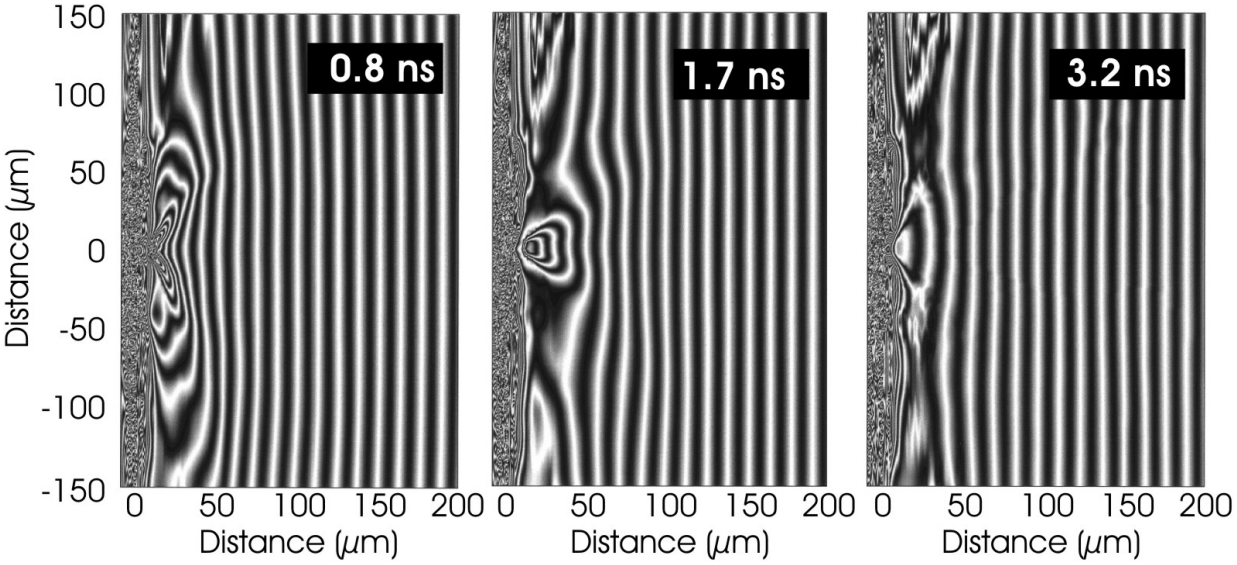

FIG. 5: Synthesized interferograms computed using the calculated electron and ion densities from Fig 3.

TABLE I: Computed "effective" real scattering factor[a] for Al at 84.4 eV.

Ion species	"Effective" f_1
Neutral (Al I)	-0.85
Ion 1 (Al II)	-4.19
Ion 2 (Al III)	-3.54
Ion 3 (Al IV)	-1.80
Ion 4 (Al V)	0.84
Ion 5 (Al VI)	3.54
Ion 6 (Al VII)	5.30
Ion 7 (Al VIII)	6.73
Ion 8 (Al IX)	8
Ion 9 (Al X)	9.18
Ion 10 (Al XI)	10
Ion 11 (Al XII)	11
Ion 12 (Al XIII)	12
Ion 13 (Al IV)	13

[a]The index of refraction $\eta = (1 - \frac{n_z f_1}{n_{crit}})^{\frac{1}{2}}$, where n_z is the density of ions with ions with charge z and n_{crit} is the critical plasma density.